

PREDICTION OF MAXIMUM EARTHQUAKE INTENSITY IN THE SAN FRANCISCO BAY REGION, CALIFORNIA,
FOR LARGE EARTHQUAKES ON THE SAN ANDREAS AND HAYWARD FAULTS

By Roger D. Borcherdt, James F. Gibbs, and Kenneth R. Lajoie

INTRODUCTION

The amount of damage resulting from the great California earthquake of April 18, 1906, varied significantly for different parts of the San Francisco Bay region. In some areas the damage was weak with "occasional fall of chimneys and damage to plaster, partitions, plumbing and the like," in other nearby areas the damage was violent with "... fairly general collapse of brick and frame structures when not unusually strong ..." (Wood, 1908). These large variations were due partly to distance from the zone of surface faulting and partly to the geologic character of the ground (compare the intensity map for San Francisco (fig. 1) with the geologic map (fig. 2)). In this paper, empirical relations are derived that quantify the dependencies of the 1906 intensities on distance and the geologic character of the ground. These relations are used to predict maximum intensities for possible future earthquakes at a scale of 1:125,000 for the San Francisco Bay region.

The San Francisco Bay region is likely to experience large earthquakes in the future. Economical reduction of the hazards associated with potential earthquakes requires delineation of areas that are especially susceptible to damage. Maps that show predicted earthquake intensity on a regional scale provide such delineations and they provide qualitative estimates of the potential hazard at specific sites. Predictions of earthquake intensity for the San Francisco Bay region are especially needed for a large earthquake on the Hayward fault. In addition, predictions of intensity for areas not developed at the time of the 1906 earthquake are needed for a large earthquake on the San Andreas fault.

The quality of the evidence for the intensities ascribed following the 1906 earthquake varied greatly. In some areas (for example, downtown San Francisco) the density of structures was sufficient to provide redundant evidence for the ascribed degree of intensity and detailed delineation of the variation in intensity levels. In less densely populated areas, intensities were ascribed on the basis of evidence observed at sites kilometres apart, with a resulting lack of detail.

In the following analyses only the intensity data from those sites (approximately one square city block in size) for which there was reliable evidence were utilized. In San Francisco (Map 19, Lawson, 1908), only those sites that were defined by Wood (1908) as having "unequivocal" evidence were considered. For the southern San Francisco peninsula (Maps 21 and 22, Lawson, 1908), only those sites intersected by an examined route were considered. On the basis of these selected 1906 intensity data, detailed geologic mapping, and comparative ground motion measurements for 99 sites, intensities can be predicted in considerably more detail than they could be ascribed following the 1906 earthquake for several areas in the San Francisco Bay region.

Two previous maps of predicted intensity have been prepared for the San Francisco Bay region (Algermissen and others, 1972; Evernden and others, 1973). The map by Algermissen and others (1972) was prepared at a scale of 1 cm \approx 7 km and is based on nonexplicit relations between intensity, distance, and site geology. Evernden and others (1973) prepared a map of predicted intensity for central California at a scale of 1 cm \approx 1.3 km and a map for the city of San Francisco at a scale of 1 cm \approx 1 km. These maps were constructed from a numerical model of the earthquake source which estimated relative peak acceleration values for a standard ground condition at various distances from the potential earthquake source; these acceleration values (a) were converted to intensity values (I) using the empirical relation

$$I = 3(0.5 + \log a).$$

The map of Evernden and others (1973) was prepared by convolving the map for uniform ground conditions with a map on which the actual geologic ground conditions

were characterized by relative intensity values determined from data of Borcherdt (1970). The numerical model was calibrated according to selected sites with good 1906 intensity data (see Evernden and others, 1973, for details).

The map prepared in this study differs from the map of Evernden and others (1973) and the map of Algermissen and others (1972) in that the predictions of intensity are based on explicit relations, derived for this study, between reliable 1906 intensity data, distance, and local geologic conditions. In addition, the predictions of intensity derived in this study require no assumptions as to numerical models of the earthquake source or relationships of peak acceleration to intensity. They are presented at a standardized map scale that permits identification of streets and other cultural features. The predicted intensities are based on a generalized geologic map recently compiled at the same scale (1:125,000) (see section at end of report on geology).

INTENSITY VS. DISTANCE

The intensities for the 1906 earthquake that were ascribed to sites on the same geologic unit generally decrease with increasing distance from the zone of surface faulting (Lawson, 1908). To quantify this apparent relation, the 1906 intensity data for the San Francisco Bay region were reconsidered on a site-by-site basis. The intensity data from only those sites (approximately one square city block in size) for which there was reliable evidence for the degree of ascribed intensity were considered. For each site underlain by the Franciscan Formation the perpendicular distance to the zone of 1906 surface faulting was measured and plotted as a function of the ascribed 1906 earthquake intensity (fig. 3). The resulting empirical relation,

$$\text{Intensity} = 2.69 - 1.90 \log(\text{distance(km)}),$$

determined by the method of least squares over the distance interval 0-15 km suggests that the ascribed intensity values for sites on the Franciscan Formation generally decrease as the logarithm of distance increases. The empirical relation shows that the intensity values decrease very rapidly with distance, with sites 3 km from the fault having observed intensities more than two intensity units smaller than those at the fault.

The sites with the highest ascribed intensities ("A", 1906 San Francisco scale) are located within 0.7 km of the center of the zone of surface rupture. For most of these sites, the unit of intensity was assigned on the basis of evidence for some form of ground failure, most of which was associated with surface faulting. The degree of intensity assigned to most of the other sites at greater distances from the fault was based on damage resulting from ground shaking or ground failures induced by ground shaking. To quantify the dependence on distance of the intensities that were due only to shaking, another empirical relation was determined with the intensity data near the fault omitted. The resulting empirical relation, $\text{Intensity} = 2.71 - 1.96 \log(\text{distance(km)})$, is essentially the same as the one determined from the complete data set. (Intensities predicted by either relation differ by 0.09 at distances less than 0.16 km and less than 0.05 for distances in the interval 0.8 to 15 km. The standard errors for the regression coefficients of the restricted and complete data sets are 0.04 and 0.03, respectively. The means and standard deviations for the samples are given in table 1.) This similarity in the derived relations suggests that the dependence of intensity on distance is not influenced by the intensities ascribed mainly on evidence of surface faulting; hence the relation determined from the complete data set is used hereafter.

INTENSITY INCREMENT VS. LOW-STRAIN AMPLIFICATION

Three components of ground motion generated by distant nuclear explosions in Nevada have been recorded

at 99 sites in the San Francisco Bay region (Borcherdt, 1970; Gibbs and Borcherdt, 1974).

Analysis of these recordings shows that certain frequencies of the low-strain ground motions are amplified considerably by certain types of local site conditions. Borcherdt (1970) showed that spectral amplification curves computed with respect to a given bedrock unit to a first approximation isolate the seismic response characteristics of the local site conditions. To isolate the dependence of the observed 1906 intensities on local site conditions (from the dependence of the intensities on distance), intensity increments were defined for each of the recording sites for which 1906 intensity data are available. The intensity increment for each site was defined as the difference between the observed intensity and the intensity predicted by the empirical relation for sites at the same distance on the Franciscan Formation (fig. 3).

The intensity increments are plotted as a function of the Average Horizontal Spectral Amplification (AHSA) values computed with respect to the Franciscan Formation from the recordings of low-strain ground motion (fig. 4) (Gibbs and Borcherdt, 1974). Empirical relations were determined (using the method of least squares) from only the data for sites in the city of San Francisco for which there was "unequivocal" evidence for the degree of ascribed 1906 intensity and from the complete data set. The two empirical relations are similar with intensity increments predicted by either relation differing by less than two-tenths (see fig. 4). The empirical relation ($\delta I = 0.27 + 2.70 \log(\text{AHSA})$) based on only the reliable intensity data in the city of San Francisco is preferred. The means and standard deviations for the samples are given in table 1. The standard error of the regression coefficient for the restricted data set is 0.29 and for the complete data set is 0.33.

The correlation coefficient of 0.95 computed for the preferred empirical relation, $\delta I = 0.27 + 2.70 \log(\text{AHSA})$, shows that a strong correlation exists between the computed intensity increments and the amplifications observed at low-strain levels. The physical meaning of this empirical correlation is complex and does not necessarily imply that amplifications observed at low-strain levels can be extrapolated directly to high-strain levels. However, there are two possible reasons for this correlation: 1) for levels of ground shaking that did not cause ground failure, the higher amplifications indicate those sites that experienced the higher levels of ground shaking and 2) for levels of ground shaking that did induce ground failure, the higher amplifications indicate those sites that were most susceptible to ground failure. In either case, the higher amplifications indicate those sites that experienced greater amounts of damage and, hence, were assigned higher degrees of intensity.

PREDICTION OF MAXIMUM EARTHQUAKE INTENSITY AT SPECIFIC SITES

Historically, large earthquakes have occurred along both the San Andreas and Hayward faults. Recent fault studies (e.g., Wesson and others, 1975) indicate a high potential exists for future large earthquakes (magnitude, 7.5-8.5) along both faults. As the types of faulting and maximum intensities for future earthquakes on the San Andreas and Hayward faults are similar, the attenuation curve for the 1906 intensities (fig. 3) may be considered useful for predicting intensities of a large earthquake on the Hayward fault as well as one on the San Andreas fault. Such predictions from the attenuation curve for the 1906 intensities (fig. 3) are valid for sites on the Franciscan Formation. For sites not on the Franciscan Formation, intensities can be predicted by using the empirical relation between intensity increment and the low-strain amplification (fig. 4). Hence, for each of the sites with measured low-strain amplifications intensities can be predicted from the two empirical curves for a large earthquake on either fault. Such predictions require only the geologic information needed to delineate the Franciscan Formation as opposed to that needed to delineate the other geologic units.

Intensities are predicted for each of the sites at which amplifications have been measured (table 1). The maximum of the intensities predicted for each site

from a large earthquake on the San Andreas fault and a large earthquake on the Hayward fault is shown on sheet 1. The map suggests that a future earthquake on either of the faults could cause as much damage at sites some distance from the faults as at sites in the immediate zones of potential surface faulting. Also, the map suggests that the earthquake hazard is not uniformly distributed throughout the San Francisco Bay region and that large variations in damage might be expected over relatively short distances. The map provides estimates of maximum earthquake intensity for the specific sites shown.

To compare the predicted intensities for an earthquake on the San Andreas with the observed 1906 intensities (table 1, cols. 8 and 9), two types of recording sites were considered. Those sites with ascribed 1906 intensities regardless of the quality of evidence were considered as one sample and those with intensities ascribed on the basis of "unequivocal" evidence were considered as another sample. (The intensity values predicted from the empirical relations based on only the reliable intensity data are plotted as a function of the observed values (fig. 5).) The mean and standard deviation of the difference between the predicted and observed values for the sites with "unequivocal" evidence are 0.03 and 0.39, respectively, and for all of the sites they are 0.06 and 0.73, respectively. The mean and standard deviation for the absolute value of the difference between the predicted and observed values are 0.29 and 0.24, respectively, for the "unequivocal" data and 0.58 and 0.43, respectively, for all the data. The larger values for the sample including all of the data are consistent with the fact that the quality of the intensity evidence is less for this sample. The mean value of 0.29 and the standard deviation 0.24 may be interpreted as indicative of the uncertainty associated with the predicted intensity values at the sites for which low-strain amplifications have been measured.

The maximum earthquake intensities are shown on sheet 1 for the sites at which low-strain amplifications have been measured. The areal density of the sites is not sufficient to draw accurate contours of equal intensity for the entire region; however, the predictions can be extrapolated to a regional scale using available geologic data.

INTENSITY INCREMENTS VS. LOCAL GEOLOGIC UNITS

The amounts of damage from numerous past earthquakes have been observed to depend strongly on the geologic character of the ground (see Duke, 1958, for a comprehensive bibliography). To investigate this dependence for the 1906 earthquake, the intensity increments computed at each of the recording sites are grouped according to the type of underlying geologic unit (table 1, col. 5) (see section on geology at end of report).

The mean of the intensity increments for each group shows that a strong correlation exists between the observed 1906 intensities and the type of geologic unit. The mean intensity increments increase with decreasing "firmness" of the geologic units showing that in general the greatest amounts of damage, excluding that in the immediate zone of surface faulting, occurred on the softest sites. These sites are in general the most likely to significantly amplify ground shaking (Borcherdt and others, 1975). In addition, these sites are the most susceptible to ground failure induced by liquefaction (Youd and others, 1975).

The means for the samples of measured intensity increments computed for the various geologic units (table 1, col. 5) were based on the intensity data from all the recording sites regardless of the quality of evidence. In the authors' opinion, an improved quantification of the intensity dependence on the geologic unit is obtained by considering the intensity increments predicted at each of the recording sites using the empirical intensity increment vs. amplification curve (fig. 4), which is based on only those intensity data for which there was unequivocal evidence. The intensity increments predicted from this curve are tabulated (table 1, col. 6), and grouped according to the type of geologic unit. The means and standard deviations for the various samples are shown at the bottom of each tabulation for the corresponding geologic unit in table 1, cols. 5 and 6. These means and standard deviations were computed for all of the

sites in each sample, including those for which it was necessary to predict the intensity increments from the analog amplifications. The means and standard deviations for the sites in each sample for which the intensity increments were predicted from the spectral amplifications are summarized in table 2. These means are preferred as a quantitative estimate of the dependence of the 1906 earthquake intensities on the geologic character of the ground.

PREDICTION OF MAXIMUM EARTHQUAKE INTENSITY ON A REGIONAL SCALE

The lack of intensity data for many areas in the San Francisco Bay region and the high vulnerability of the region to earthquakes define a need for intensity predictions on a regional basis. To make regional predictions, a generalized geologic map was compiled at a scale of 1:125,000 (sheet 3). The map delineates the geologic units determined to have significantly different seismic responses (Gibbs and Borcherdt, 1974) (see section on geology).

Utilizing the mean intensity increments for the generalized geologic units predicted on the basis of the reliable 1906 intensity data (table 2), the empirical intensity vs. distance relation (fig. 3), and the generalized geologic map, intensities were predicted on a regional basis (map sheet 2). The intensity shown for each area on the map is the maximum of those predicted for a large earthquake on the San Andreas fault and a large earthquake on the Hayward fault. The standard deviations computed for the samples of predicted intensity increments associated with the various geologic units (table 2) are indicative of the variability associated with the predictions. Areas are delineated on the map according to the grades of predicted intensity defined by the San Francisco intensity scale. Use of the San Francisco scale reduces uncertainties in the predictions that would result from conversion to another intensity scale. Conversion to another intensity scale would be based implicitly on intensity data from other areas. Comparisons between the Rossi-Forel scale, the San Francisco scale, and the Modified Mercalli scale as presented by Wood (1908), Wood and Newmann (1931), and Richter (1958), are presented in figure 6.

Some of the boundaries between areas on the map with different predicted intensities coincide with geologic boundaries; others were defined by the minimum perpendicular distance of the underlying geologic unit from the faults. The map predicts zones of "very violent" ("A") intensity for linear zones along the faults and for areas relatively close to the faults underlain by bay mud. The widths of the "very violent" zones along the faults vary depending on the type of neighboring geologic unit. The widest zones occur in areas along the faults underlain by alluvium.

The map (sheet 2) shows more detail in some areas than does the 1906 intensity map. This is especially true for areas south of the city of San Francisco (Maps 21 and 22, Lawson, 1908). The greater detail in some areas is due to the detailed geologic information currently available and to the scarcity of 1906 intensity data. The map delineates potentially hazardous areas during large earthquakes and shows, as did the 1906 intensity maps, that earthquake hazards are not uniformly distributed throughout the San Francisco Bay region.

SUMMARY

The apparent dependencies of the 1906 earthquake intensities on the geologic character of the ground and distance from the zone of surface faulting have been quantified using only reliable 1906 intensity data.

The empirical relation derived between intensity and perpendicular distance to the fault for 917 sites (approximately one square city block in size) on the Franciscan Formation is

$$\text{Intensity} = 2.69 - 1.90 \log(\text{distance}(\text{km})).$$

Omission of the intensity data due to surface faulting did not influence this intensity vs. distance relation. Intensity increments between the observed intensity and that predicted by this attenuation relation correlate strongly with the measured low-strain amplifications of ground motion generated by nuclear explosions in Nevada. The empirical relation derived between the

low-strain amplifications and the intensity increments is

$$\text{Intensity Increment} = 0.27 + 2.70 \log(\text{AHSA}).$$

This empirical relation was derived from the data at the 11 recording sites for which "unequivocal" evidence exists for the ascribed degree of 1906 intensity.

The intensity values predicted at the low-strain recording sites (map sheet 1) using the two preceding empirical relations are based on reliable 1906 intensity data. The prediction of these values did not require any geologic data except that which describes the Franciscan Formation. These values provide estimates of the maximum intensity that the specific sites might experience during future large earthquakes. Extension of these predictions to the entire region requires incorporation of additional geologic data. The intensity values predicted at the specific sites (map sheet 1) for a large earthquake on the San Andreas fault show good agreement with those actually ascribed following the 1906 earthquake. The means and standard deviations for the magnitude of the difference between the predicted and observed intensity values for 46 sites are 0.58 and 0.43, respectively.

The average intensity increments derived for the various geologic units provide a quantitative estimate of the dependence of the 1906 intensities on the geologic character of the ground. These average intensity increments provide the basis for predicting earthquake intensities on a regional scale. The means and standard deviations derived for the various geologic units are summarized in table 2.

The map showing maximum earthquake intensity on a regional scale (map sheet 2) is based on the derived attenuation curve for the intensities of the 1906 earthquake, the average intensity increments derived for the various geologic units, and a generalized geologic map compiled at a scale of 1:125,000. The map delineates potentially hazardous areas during a large earthquake on either the San Andreas or Hayward fault. For a large earthquake on the San Andreas fault, the map defines several potentially hazardous areas in addition to those defined by the original 1906 intensity maps. The map provides a crude form of seismic zonation for a part of the San Francisco Bay region and it should be useful for development of certain general land-use policies for reducing the hazards associated with potential earthquakes. However, the map does not necessarily define the specific nature of the hazard in each area; for example, in areas underlain by bay mud the map does not distinguish between intensities that may be high because of damage induced directly by strong ground shaking and those that may be high because of ground failures associated with liquefaction. As a result the map is useful only for development of general land-use policies. More detailed construction policies must be based on individual site investigations and specific maps such as those showing active faults (Wesson and others, 1975), liquefaction potential (Youd and others, 1975), and landslide susceptibility (Nilsen and Brabb, 1975).

REFERENCES CITED

- Algermissen, S. T. (principal investigator), 1972, A study of the earthquake losses in the San Francisco Bay Area: NOAA report, 220 p.
- Borcherdt, R. D., 1970, Effects of local geology on ground motion near San Francisco Bay: *Seismol. Soc. America Bull.*, v. 60, p. 29-61.
- Borcherdt, R. D., Joyner, W. B., Warrick, R. E., and Gibbs, J. F., 1975, Response of local geologic units to ground shaking, in *Studies for seismic zonation of the San Francisco Bay region*: U.S. Geol. Survey Prof. Paper 941A.
- Duke, C. M. (compiler), 1958, Bibliography of effects of soil conditions on earthquake damage: *Earthquake Eng. Inst.* 47.
- Evernden, J. F., Hibbard, R. R., and Schneider, J. F., 1973, Interpretation of seismic intensity data: *Seismol. Soc. America Bull.*, v. 63, p. 399-422.
- Gibbs, J. F., and Borcherdt, R. D., 1974, Effects of local geology on ground motion in the San Francisco Bay region--a continued study: U.S. Geol. Survey open-file report 74-222.
- Lawson, A. C. (chairman), 1908, The California earthquake of April 18, 1906, Report of the State

- Earthquake Commission: Carnegie Inst. Washington Pub. 87, Washington, D.C.
- Nilsen, T. H., and Brabb, E. E., 1975, Landslides, in Studies for seismic zonation of the San Francisco Bay region: U.S. Geol. Survey Prof. Paper 941A.
- Richter, C. F., 1958, Elementary seismology: W. H. Freeman and Co., San Francisco, Calif., 768 p.
- Schlocker, J., Bonilla, M. G., and Radbruch, D. H., 1958, Geology of the San Francisco north quadrangle, California: U.S. Geol. Survey Misc. Geol. Inv. Map I-272.
- Wesson, R. L., Helley, E. J., Lajoie, K. R., and Wentworth, C. M., 1975, Faults and future earthquakes, in Studies for seismic zonation of the San Francisco Bay region: U.S. Geol. Survey Prof. Paper 941A.
- Wood, H. O., 1908, Distribution of apparent intensity in San Francisco, in The California earthquake of April 18, 1906, Report of the State Earthquake Investigation Commission: Carnegie Inst. Washington Pub. 87, Washington, D.C., p. 220-245.
- Wood, H. O., and Newmann, F., 1931, Modified Mercalli intensity scale of 1931: Seismol. Soc. America Bull., v. 53, p. 979-987.
- Youd, T. L., Nichols, D. R., Helley, E. J., and Lajoie, K. R., 1975, Liquefaction potential, in Studies for seismic zonation of the San Francisco Bay region: U.S. Geol. Survey Prof. Paper 941A.

SAN FRANCISCO INTENSITY SCALE FOR 1906 EARTHQUAKE

The following grades of apparent intensity were ascribed by H. O. Wood (1908, p. 224-225) in the city of San Francisco after the California earthquake of April 18, 1906.

- Grade A. Very violent - Comprises the rending and shearing of rock masses, earth, turf, and all structures along the line of faulting; the fall of rock from mountainsides; numerous landslips of great magnitude; consistent, deep, and extended fissuring in natural earth; some structures totally destroyed.
- Grade B. Violent - Comprises fairly general collapse of brick and frame buildings when not unusually strong; serious cracking of brickwork and masonry in excellent structures; the formation of fissures, step faults, sharp compression anticlines, and broad, wavelike folds in paved and asphalt-coated streets, accompanied by the ragged fissuring of asphalt; the destruction of foundation walls and underpinning structures by the undulation of the ground; the breaking of sewers and water mains; the lateral displacement of streets; and the compression, distension, and lateral waving or displacement of well-ballasted streetcar tracks.
- Grade C. Very strong - Comprises brickwork and masonry badly cracked, with occasional collapse; some brick and masonry gables thrown down; frame buildings lurching or listing on fair or weak underpinning structures, with occasional falling from underpinning or collapse; general destruction of chimneys and of masonry, brick, or cement veneers; considerable cracking or crushing of foundation walls.
- Grade D. Strong - Comprises general but not universal fall of chimneys; cracks in masonry and brickwork; cracks in foundation walls, retaining walls, and curbing; a few isolated cases of lurching or listing of frame buildings built upon weak underpinning structures.
- Grade E. Weak - Comprises occasional fall of chimneys and damage to plaster, partitions, plumbing, and the like.

Generalized map

A generalized geologic map of the southern bay region (sheet 3) provided the means of extrapolating predictions of maximum earthquake intensities, at the 99 nuclear explosion recording sites (sheet 1) to a regional scale (sheet 2). The numerous geologic formations in the southern bay region were grouped into seven map units on the basis of seismic response (Gibbs and Borchardt, 1974; also see table 1, col. 4) and physical similarities. The seven map units are not rigorously defined and may be further subdivided in the future with more complete seismic data.

Most of the geologic units are not homogeneous. Each has a range in characteristics, such as lithology, degree of induration, structure, thickness, and depth of weathering, which, along with other factors, such as geometry, topography, and depth to the ground water table, undoubtedly affect seismic response. The predicted maximum intensity zones (sheet 2) derived from the generalized geologic map (sheet 3) represent an average of these variables. Therefore, the maximum intensity at any particular site may vary from that indicated on map sheet 2 due to local geologic conditions.

Faults

Sudden displacement on five faults within the southern San Francisco Bay region could generate earthquakes of magnitude 7.0 or greater (Wesson and others, 1975). These faults are the Seal Cove-San Gregorio (M 7.4), the San Andreas (M 8.5), the Sargent (M 7.4), the Hayward (M 7.5), and the Calaveras (M 7.3). Maximum earthquake intensities could be predicted on a regional basis for large earthquakes on each of these faults. In this study predictions of maximum intensity were made only for large earthquakes on the San Andreas and Hayward faults. These faults are historically the most active and, because of their locations, they would most likely generate the maximum intensities in the densely populated alluvial lowland of the southern bay region.

The Hayward fault does not extend southeastward beyond Evergreen Valley east of San Jose. The intensity predictions south of San Jose were made using the Quimby, Silver Creek, and Coyote Creek faults mainly because they form a natural extension of the Hayward fault as the eastern bounding Quaternary fault in the southern Santa Clara Valley area. Wesson and others (1975) indicate the Silver Creek fault is probably active (fault creep and small earthquakes) and capable of generating earthquakes of magnitude 6.2. There is no implication, however, that there will be simultaneous movement on these faults if there is movement generating a large earthquake on the Hayward fault. Data compiled by Wesson and others (1975) suggest that the Calaveras fault, which lies 1.5-5.5 km east of the Silver Creek and Coyote Creek faults, is the most likely fault to generate large earthquakes (M 7.3) in the southeastern Santa Clara Valley area.

Table 1

HORIZONTAL AMPLIFICATIONS, INTENSITY INCREMENTS (MEASURED AND PREDICTED) AND INTENSITIES (MEASURED (1906) AND PREDICTED)
FOR LOW-STRAIN RECORDING SITES TOGETHER WITH MEANS AND STANDARD DEVIATIONS FOR VARIOUS SAMPLES***

Recording site identification	Distance (km)		Horizontal amplification wrt Franciscan	Intensity increment wrt Franciscan		Earthquake intensities (S.F. scale)		
	San Andreas	Hayward		Measured	Predicted	Hayward Predicted	San Andreas Predicted	Observed
SURFACE LAYER--BEDROCK (granite)								
H16	2.90	32.83	0.60	-0.19	-0.32	-0.51	1.49	2.0
I16	7.89	37.66	0.50	-0.99	-0.53	-0.83	0.45	0.0
H17	4.83	34.92	0.72	-0.39	-0.11	-0.35	1.28	1.0
P17	7.89	37.66	0.55	-0.99	-0.44	-0.74	0.55	0.0
RI7	7.08	36.21	<u>0.77</u>	<u>-1.08</u>	<u>-0.04</u>	<u>-0.31</u>	<u>1.04</u>	<u>0.0</u>
Mean			0.63	-0.65	-0.29	-.55	0.96	0.60
Standard deviation			0.11	.55	0.21	.23	.45	.89
SURFACE LAYER--BEDROCK (Franciscan Formation)								
BLM	0.64	28.00	1.24	-0.05	0.53	0.47	3.58	3.0
GGP	7.24	22.69	0.81	0.94	0.03	0.14	1.08	2.0
J5*	14.65	15.93	0.82	0.52	0.03	0.44	0.51	1.0**
I7	14.65	15.61	0.82	-0.48	0.03	0.46	0.51	0.0**
J7	14.65	15.93	0.65	0.52	-0.23	0.18	0.25	1.0**
I8	14.65	15.61	0.85	-0.48	0.08	0.50	0.56	0.0**
LI1	8.21	22.21	0.80	0.05	0.02	0.15	0.97	1.0
K16	4.18	25.43	0.75	0.49	-0.06	-0.04	1.45	2.0
LI6	2.41	27.20	1.24	0.04	0.52	0.49	2.48	2.0
Q16	1.77	27.68	1.39	0.78	0.66	0.61	2.87	3.0
T16	1.93	31.70	1.58	<u>-0.15</u>	<u>0.81</u>	<u>0.65</u>	<u>2.95</u>	<u>2.0</u>
Mean				.20	.22	.37	1.56	1.55
Standard deviation				.48	.34	.22	1.19	1.04
K1	21.40	8.69	0.46		-0.63	0.28	-0.46	---
S17	31.70	1.77	1.46		0.72	2.94	0.56	---
CYH	21.40	8.85	<u>0.50</u>		<u>-0.55</u>	<u>0.34</u>	<u>0.51</u>	---
Mean			.96		.14	.54	1.27	
Standard deviation			.36		.45	.72	1.21	
SURFACE LAYER--BEDROCK (Santa Clara Formation)								
P1	4.83	24.94	1.49	0.61	0.74	0.78	2.14	2.0
P2	4.83	24.94	1.12	0.61	0.40	0.44	1.79	2.0
K9	4.18	23.17	2.09	0.49	1.14	1.24	2.65	2.0
K17	4.51	22.05	2.17	0.55	1.18	1.32	2.63	2.0
LI7	0.48	30.26	0.87	-0.29	0.11	-0.01	3.40	3.0
Q17	6.76	21.24	<u>2.48</u>	<u>1.89</u>	<u>1.34</u>	<u>1.51</u>	<u>2.45</u>	<u>3.0</u>
Mean			1.70	.64	.82	.88	2.51	2.33
Standard deviation			.64	.70	.49	.59	.54	.52
SURFACE LAYER--BEDROCK (Page Mill Basalt)+								
L3*	5.63	24.14	2.13	0.74	1.16	1.23	2.42	2.0
J4*	6.12	23.66	<u>1.94</u>	<u>1.80</u>	<u>1.05</u>	<u>1.13</u>	<u>2.25</u>	<u>3.0</u>
Mean			2.04	1.27	1.11	1.18	2.34	2.5
Standard deviation			.13	.75	.08	.07	.12	.71

Table 1--Continued

HORIZONTAL AMPLIFICATIONS, INTENSITY INCREMENTS (MEASURED AND PREDICTED) AND INTENSITIES (MEASURED (1906) AND PREDICTED) FOR LOW-STRAIN RECORDING SITES TOGETHER WITH MEANS AND STANDARD DEVIATIONS FOR VARIOUS SAMPLES***

Recording site identification	Distance (km)		Horizontal amplification wrt Franciscan	Intensity increment		Earthquake intensities (S.F. scale)		
	San Andreas	Hayward		Measured	Predicted	Hayward Predicted	San Andreas Predicted	Observed
SURFACE LAYER--BEDROCK (serpentine and ultramafic rocks)								
H9	2.09	28.00	1.56	-0.08	0.80	0.74	2.88	2.0
J16	0.16	29.61	<u>0.66</u>	<u>-1.19</u>	<u>-0.22</u>	<u>-0.32</u>	<u>3.98</u>	<u>3.0</u>
Mean			1.11	-.64	.29	.21	3.43	2.50
Standard deviation			.64	.78	.72	.75	.78	.71
SURFACE LAYER--BEDROCK (Great Valley sequence and Tertiary rocks)								
Q13*	31.38	4.35	1.21		0.50	1.98	0.35	
Q14*	32.99	4.83	0.87		0.10	1.50	-0.09	
P19*	36.05	6.12	1.25		0.53	1.73	0.27	
R19*	34.44	5.15	2.44		1.32	2.66	1.09	
T19*	33.96	4.51	1.55		0.79	2.24	0.57	
19B*	5.63	35.89	1.16		0.45	0.19	1.71	
19C*	2.90	32.83	1.63		0.84	0.66	2.66	
19E*	4.99	34.44	1.21		0.50	0.27	1.86	
19W*	7.56	37.34	<u>1.49</u>		<u>0.74</u>	<u>0.45</u>	<u>1.76</u>	
Mean			1.42		.64	1.30	1.13	
Standard deviation			.45		.34	.93	.92	
SURFACE LAYER--ALLUVIUM								
J1*	8.85	20.92	2.37	2.11	1.29	1.47	2.18	3.0
H2*	11.10	18.51	1.56	2.29	0.80	1.08	1.50	3.0
K2	13.20	16.25	1.49	2.44	0.74	1.13	1.30	3.0
Q2	9.17	20.44	1.12	2.14	0.40	0.61	1.27	3.0
T2*	4.51	25.43	1.69	1.55	0.89	0.91	2.34	3.0
H4*	5.95	23.66	2.07	1.78	1.12	1.21	2.34	3.0
K4*	9.33	18.99	1.63	2.15	0.84	1.11	1.69	3.0
K5	12.39	17.86	2.76	1.38	1.46	1.78	2.08	2.0**
K7	12.39	17.86	2.23	1.38	1.22	1.53	1.83	2.0**
R7	14.16	16.09	1.29	0.49	0.57	0.97	1.08	1.0**
H8	10.94	18.67	3.10	2.28	1.60	1.88	2.32	3.0
J8	5.47	24.62	1.86	1.71	1.00	1.05	2.29	3.0
K8	7.56	22.21	3.14	1.98	1.61	1.75	2.64	3.0
L8	7.08	20.60	3.47	1.92	1.73	1.93	2.81	3.0
J11	5.63	24.78	1.20	-0.26	0.49	0.53	1.75	1.0
K11	10.46	20.12	0.82	0.25	0.04	0.26	0.80	1.0
Q11	1.61	28.81	3.60	1.70	1.78	1.70	4.07	4.0
T11	4.51	25.75	3.29	0.55	1.67	1.68	3.12	2.0
L19*	2.74	27.84	2.17	<u>0.14</u>	<u>1.18</u>	<u>1.13</u>	<u>3.04</u>	2.0
Mean				1.47	1.08	1.25	2.13	
Standard deviation				.83	.50	.48	.80	
I4*	24.46	5.79	2.19		1.19	2.43	1.25	
R8*	19.47	7.24	1.18		0.47	1.53	0.71	
T8	14.32	13.68	4.67		2.08	2.61	2.58	
L9	8.85	17.86	3.92		1.87	2.19	2.77	
S12*	17.06	11.59	0.86		0.10	0.77	0.45	
W15*	27.84	2.74	2.07		1.13	2.99	1.08	
I18	13.36	13.52	2.72		1.45	1.99	2.00	
K18	23.17	4.83	3.63		1.78	3.18	1.88	
L18	16.25	10.14	2.32		1.26	2.04	1.65	
P18	18.83	7.56	2.84		1.50	2.52	1.77	
S18	17.06	9.50	3.24		1.65	2.49	2.00	
T18	21.40	4.99	<u>5.03</u>		<u>2.17</u>	<u>3.53</u>	<u>2.33</u>	
Mean			2.44	1.47	1.20	1.68	1.96	2.53
Standard deviation			1.09	.83	.57	.80	.79	.84

Table 1--Continued

HORIZONTAL AMPLIFICATIONS, INTENSITY INCREMENTS (MEASURED AND PREDICTED) AND INTENSITIES (MEASURED (1906) AND PREDICTED)
FOR LOW-STRAIN RECORDING SITES TOGETHER WITH MEANS AND STANDARD DEVIATIONS FOR VARIOUS SAMPLES***

Recording site identification	Distance (km)		Horizontal amplification wrt Franciscan	Intensity increment wrt Franciscan		Earthquake intensities (S.F. scale)		
	San Andreas	Hayward		Measured	Predicted	Hayward Predicted	San Andreas Predicted	Observed
SURFACE LAYER--BAY MUD								
P5	14.81	15.45	6.43	2.53	2.46	2.89	2.92	3.0**
Q5	14.97	15.29	7.15	2.54	2.58	3.02	3.04	3.0**
T5*	14.16	16.42	7.50	1.49	2.64	3.02	3.14	2.0
H7	14.32	15.77	4.02	2.50	1.90	2.32	2.40	3.0
P7	14.81	15.45	5.45	2.53	2.26	2.70	2.73	3.0**
T7	13.04	17.54	7.39	2.43	2.62	2.95	3.19	3.0**
Mean				2.34	2.41	2.82	2.90	2.83
Standard deviation				.42	.29	.27	.30	.41
H1	14.48	15.61	4.84		2.12	2.55	2.61	
Q1	11.27	18.67	5.52		2.28	2.55	2.97	
T1	19.96	10.30	3.41		1.71	2.48	1.94	
R2*	10.78	18.83	3.44		1.72	1.99	2.45	
H3*	13.20	16.74	5.75		2.33	2.69	2.89	
K3*	13.84	15.93	5.31		2.23	2.64	2.76	
L4*	13.84	15.77	2.69		1.43	1.85	1.96	
P4*	7.89	21.89	2.88		1.51	1.66	2.50	
Q4	9.66	20.60	5.21		2.21	2.41	3.03	
R4*	18.99	11.43	8.56		2.79	3.47	3.06	
I5A	10.14	20.12	16.25		3.54	3.76	4.32	
I5B	9.66	20.60	13.75		3.35	3.54	4.17	
I5C	8.69	21.57	12.29		3.22	3.38	4.12	
R5	10.46	19.96	9.13		2.87	3.09	3.62	
T9	21.56	6.76	6.75		2.51	3.63	2.67	
I11	14.48	15.61	6.43		2.46	2.88	2.94	
Q12*	26.55	3.06	1.73		0.92	2.69	0.91	
L ₁ 14*	20.28	9.01	3.28		1.67	2.55	1.88	
L ₂ 14*	19.96	9.33	5.54		2.28	3.13	2.50	
L ₃ 14*	19.63	9.66	2.86		1.50	2.32	1.74	
L ₄ 14*	19.31	9.98	3.53		1.75	2.55	2.00	
L ₅ 14*	18.99	10.30	3.48		1.74	2.50	2.00	
L ₆ 14*	18.67	10.62	2.91		1.52	2.27	1.80	
H15*	22.21	7.56	3.12		1.61	2.63	1.74	
H18*	24.78	5.63	4.19		1.95	3.22	2.00	
Q18	24.62	5.79	2.55		1.37	2.61	1.42	
R18	23.50	6.76	3.74		1.82	2.94	1.91	
Mean			5.67		2.15	2.75	2.59	
Standard deviation			3.31		.61	.49	.79	

*Predicted intensities determined from analog amplifications.

**Observed intensity San Francisco scale. For other sites observed intensity was Rossi Forel Scale which was converted to San Francisco Scale, X ↔ 4.0, IX ↔ 3.0, VIII-IX ↔ 2.0, VII-VIII ↔ 1.0, VI-VII ↔ 0.0, where 4.0 to 0.0 is equivalent to A through E.

***Means and standard deviations are computed for samples including sites with analog amplifications as well as those sites with spectral amplifications. See Gibbs and Borchardt (table 3, 1974) for means and standard deviations computed for samples including only those sites with spectral amplifications.

†These sites are located on the boundary of Page Mill Basalt and Santa Clara Formation.

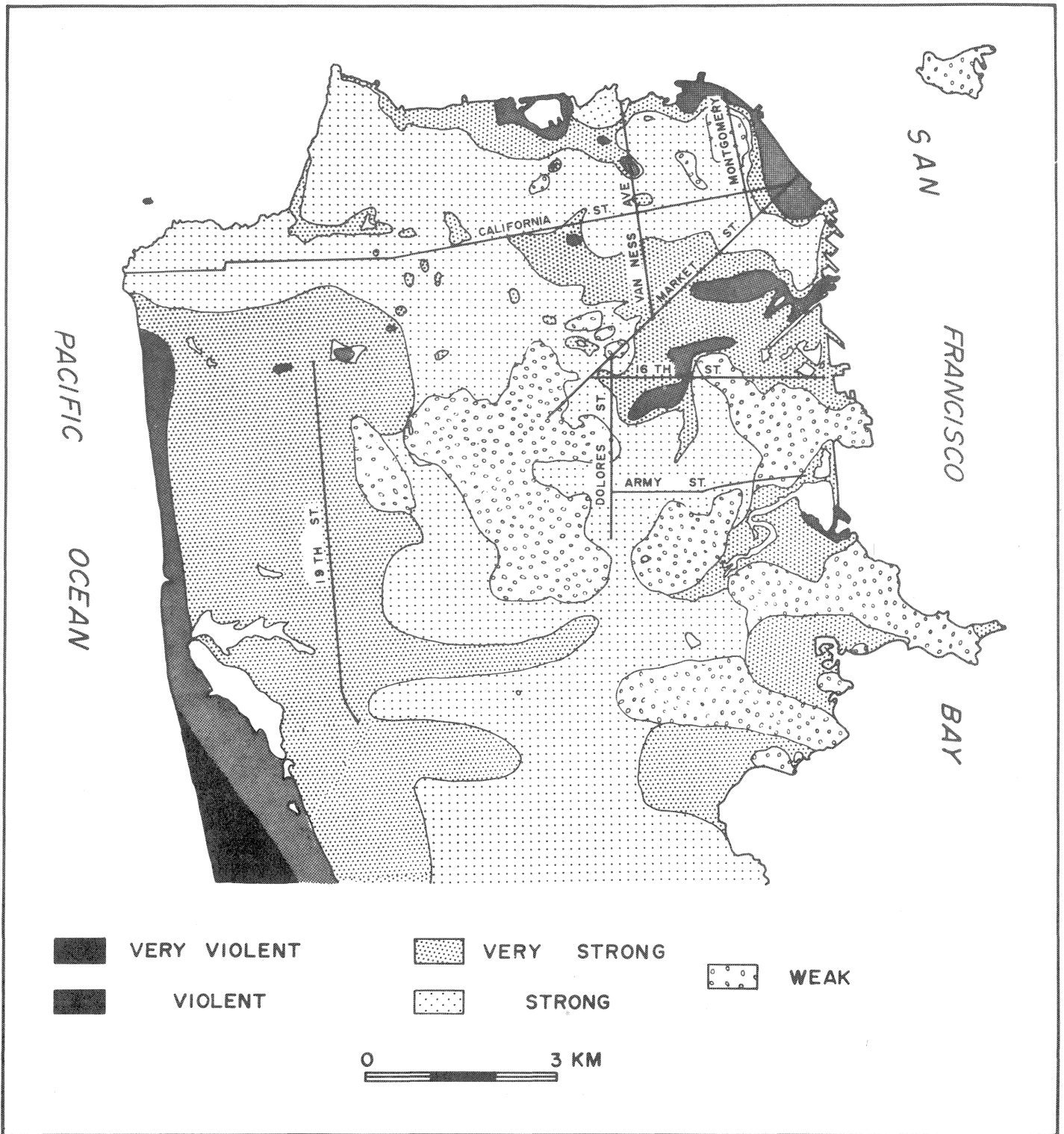


Figure 1. Apparent intensity of the 1906 earthquake in San Francisco, Calif. (see section entitled "San Francisco Intensity Scale for 1906 Earthquake" for detailed description) (after Wood, 1908).

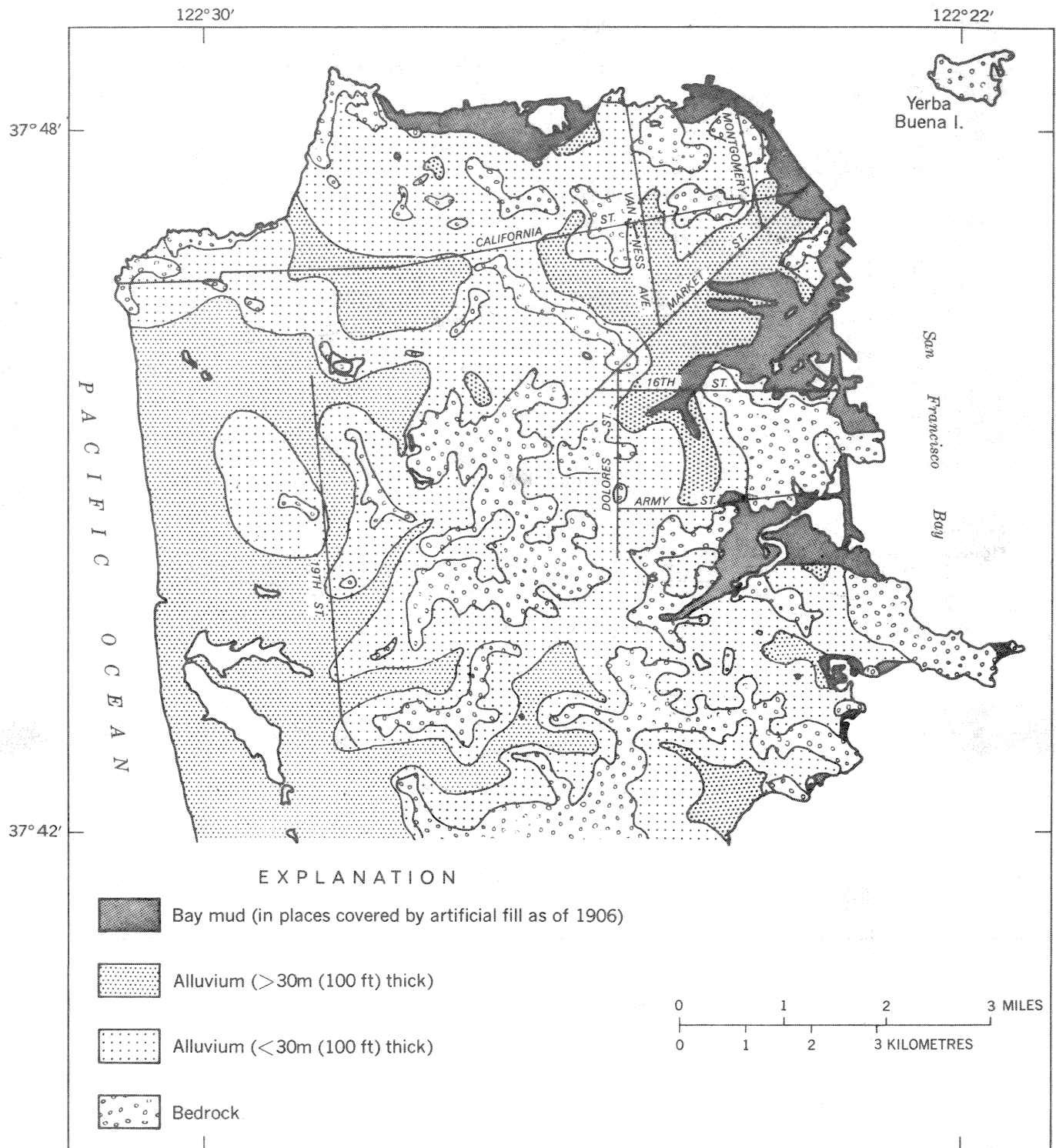


Figure 2. Generalized geologic map of San Francisco, Calif. Compiled by K. R. Lajoie from data of Schlocker and others (1958).

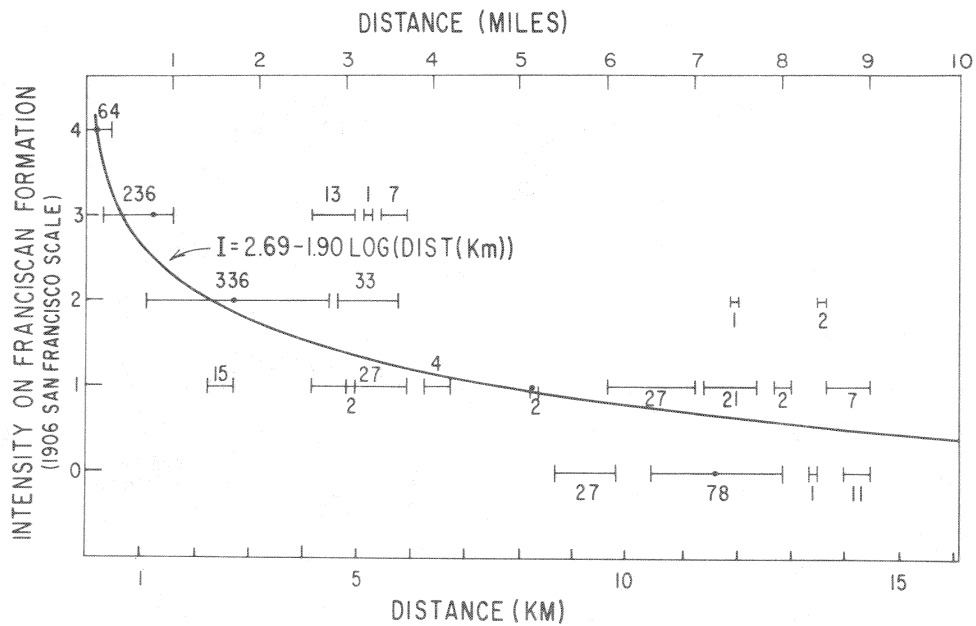


Figure 3.--Observed intensity of the 1906 earthquake in relation to perpendicular distance from the zone of surface rupture for sites (one square city block in size) underlain by the Franciscan Formation. For sites with "unequivocal" evidence in San Francisco (Map 19, Lawson, 1908), the number of observed intensity values is shown below the corresponding distance interval. For sites intersected by an "examined route" south of San Francisco (Maps 21 and 22, Lawson, 1908), the number of observed intensities is shown above the corresponding distance interval. The observed 1906 intensities are expressed in terms of the San Francisco intensity scale with the letters A-E corresponding to the numbers 4-0, respectively.

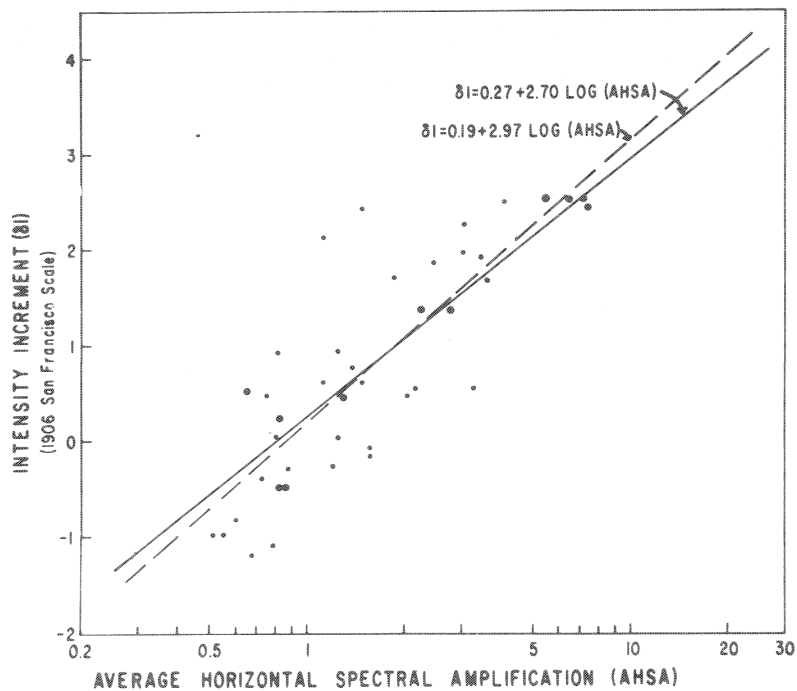


Figure 4.--Intensity increments in relation to average horizontal spectral amplification computed at corresponding sites from recordings of nuclear explosions. Both the intensity increment values and the average horizontal spectral amplification values were computed with respect to the corresponding average value determined for sites underlain by the Franciscan Formation. The empirical relation ($\Delta I = 0.19 + 2.97 \text{ log}(\text{AHSA})$) is based on the data from all the recording sites for which there was an observed 1906 intensity value (small dots). The empirical relation ($\Delta I = 0.27 + 2.70 \text{ log}(\text{AHSA})$) is based on only the data from sites in San Francisco for which there was unequivocal evidence for the ascribed degree of 1906 intensity (large dots).

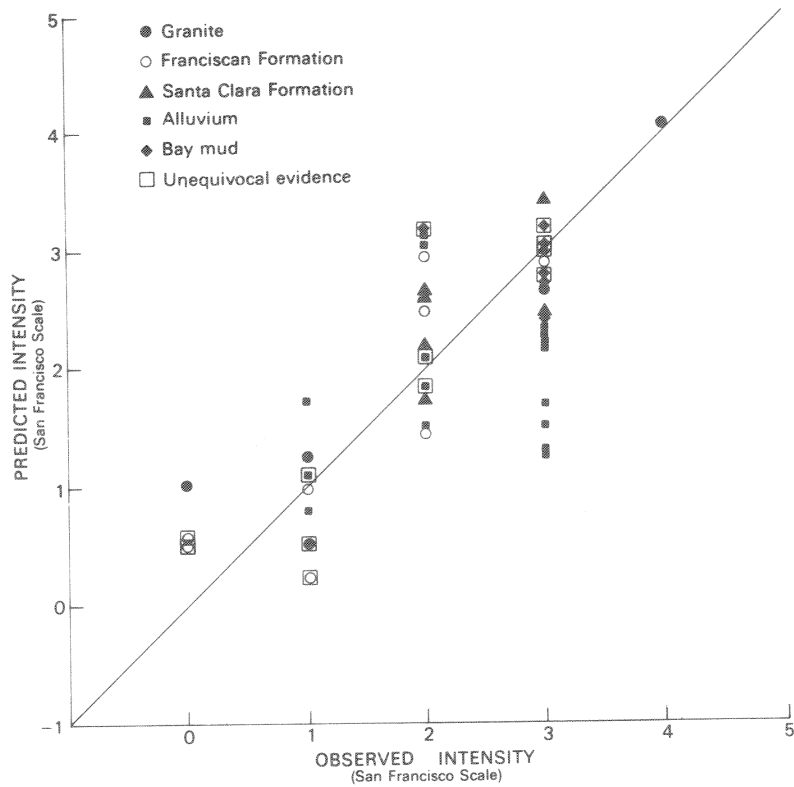


Figure 5.--Observed 1906 intensity values for the low-strain recording sites in relation to the intensity values for an earthquake on the San Andreas fault predicted on the basis of the empirical relations derived from only the reliable 1906 intensity data (empirical relations shown in figs. 3 and 4). The line shown with zero intercept and unit slope provides a base line for comparing the observed and predicted values (numbers 4-0 correspond to letters A-E, respectively, of San Francisco intensity scale).

A		B	
San Francisco scale	Rossi-Forel scale	Rossi-Forel scale	Modified Mercalli scale
Grade A	10	10	X-XII
		9+	IX
Grade B	9	8+ to 9-	VIII
		8-	VII
Grade C	8	6 to 7	VI
Grade D	7		
Grade E			

Figure 6.--Comparison of earthquake intensity scales. A, Comparison of San Francisco scale and Rossi-Forel scale presented by Wood (1908, p. 226). B, Comparison of Rossi-Forel scale and Modified Mercalli scale presented by Wood and Neumann (1931, p. 280-281) and Richter (1958, p. 651).

